

Validation of a NaI(Tl) and LaBr₃(Ce) detector's models via measurements and Monte Carlo simulations

I. Mouhti^a, A. Elanique^{a,*}, M.Y. Messous^b, B. Belhorma^b, A. Benahmed^c

^a Laboratory of Condensed Matter and Nanomaterials for Renewable Energy Faculty of Sciences, University Ibn Zohr Agadir, Morocco

^b Material Sciences Unit-DERS, National Center for Energy, Sciences and Nuclear Techniques, CNESTEN, Rabat, Morocco

^c Instrumentation Development Unit-DERS, National Center for Energy, Sciences and Nuclear Techniques, CNESTEN, Rabat, Morocco

ABSTRACT

This work relates to the study and characterization of the response function of two scintillation detectors with similar size: 2" × 2" NaI(Tl) and 2" × 2" LaBr₃(Ce). The photon detection efficiency and energy resolution curve were measured for the NaI(Tl) detector in the gamma energy range from 60 keV to 1408 keV. A precise mathematical model of the two scintillators was developed using the Monte Carlo simulation code MCNP. Comparison of the efficiency data with MCNP simulations showed good agreement enabling the validation of the computational models for both NaI(Tl) and LaBr₃(Ce) detectors.

1. Introduction

Lanthanum Bromide LaBr₃(Ce) inorganic scintillator is a new type of nuclear detector used in gamma spectrometric systems. It is becoming an attractive alternative to the conventional NaI(Tl) detector because of its promising intrinsic performances: Compared to NaI(Tl) detector, the LaBr₃(Ce) scintillator has many useful characteristics: improved energy resolution (3% at 662 keV), fast time response (decay constant of circa 26 ns) enabling high count rate applications, high gamma detection efficiency, operation at room temperature and promising technology for manufacturing crystal at larger sizes.

However, the main drawback of LaBr₃(Ce) detector is its intrinsic activity due to the presence of ¹³⁸La radioisotope (0.09% natural abundance) (Knoll, 2000): a gamma rays of 1435.8 keV and 788 keV are being produced during the decay of the ¹³⁸La (Saizu & Cata-Danil, 2011; Sonzogni, 2003). Typically, such intrinsic background is about 1–2 counts/cm³. s. Another limiting factor is that LaBr₃(Ce) is more hygroscopic than NaI(Tl) and require much more attention during the growth process. Consequently, the cost of manufacturing becomes more expensive relative to NaI(Tl) (Knoll, 2000).

This work aims to perform a comparative study between performances of two inorganic crystals of similar size: a classical 2" × 2" NaI(Tl) detector and an 2" × 2" LaBr₃(Ce) detector's model. We first have characterized experimentally the 2" × 2" NaI detector and validated its mathematical model by using Monte Carlo (MC) simulations. Secondly, we have developed a MC model for the 2" × 2" cylindrical LaBr₃(Ce)

detector for which data were extracted from (Casanovas et al., 2012).

Validation of both NaI(Tl) and LaBr₃(Ce) detector's model was based on the comparison of the experimental efficiency curve, in the gamma ray energy range up 1408 keV, with the computed one using the MC code (Ewa et al., 2001). The energy resolution function was determined experimentally and used to improve the simulated spectra.

2. Material and methods

2.1. Experimental setup

Experimental characterization of the NaI(Tl) crystal was performed using standard gamma spectrometry equipment. Fig. 1 shows a schematic representation of the experimental setup used to carry out the efficiency measurements. The NaI(Tl) detector output was connected to a delay line amplifier (DLA). This amplifier was used to avoid the baseline shift. The bipolar output of the DLA was then directed to a multichannel analyser (MCA), in order to acquire the energy spectrum for each gamma source.

The 2" × 2" cylindrical NaI(Tl) detector used in the present work was produced by BICRON. It was coupled to a preamplifier (BICRON Model 2M2/2) and an amplifier (TENNELEC Model 952A), which were connected to a multichannel pulse-height analyser (Multiport II CANBE-RRA). The NaI(Tl) crystal was irradiated with four radioactive sources namely: ²⁴¹Am, ⁶⁰Co, ¹⁵²Eu and ¹³⁷Cs for which main features have been shown in Table 1.

Peer review under responsibility of The Egyptian Society of Radiation Sciences and Applications.

* Corresponding author.

E-mail address: elanique01@yahoo.com (A. Elanique).

<https://doi.org/10.1016/j.jrras.2018.06.003>

Received 20 March 2018; Received in revised form 5 June 2018; Accepted 7 June 2018

Available online 19 June 2018

1687-8507/ © 2018 The Egyptian Society of Radiation Sciences and Applications. Published by Elsevier B.V. This is an open access article under the CC BY-NC-ND license (<http://creativecommons.org/licenses/by-nc-nd/4.0/>).

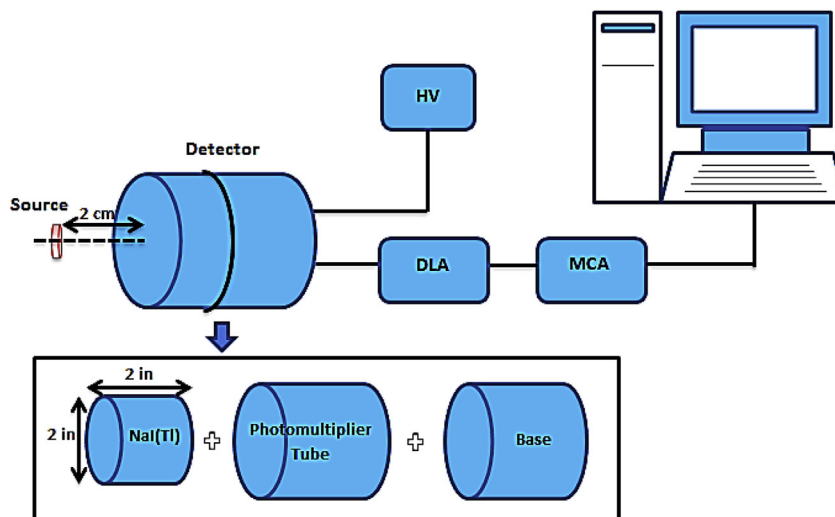


Fig. 1. Schematic representation of the experimental setup used for efficiency measurements.

Table 1

Information data of the sources used in the experiment. Photon intensities are indicated in percent (%).

Current activity (kBq)	Photon energy (keV)	Half-Live (year)	Radionuclide
2401.20	59.54 (36.0%)	432.2	²⁴¹ Am
5.10	1173.24 (99.87%)	5.27	⁶⁰ Co
	1332.51 (99.98%)		
118.52	121.78 (28.31%)	13.53	¹⁵² Eu
	244.69 (7.55%)		
	344.27 (26.59%)		
	1112.07 (13.41%)		
	1408.01 (20.85%)		
121.04	661.65 (84.6%)	30.07	¹³⁷ Cs

The spectrum analysis software that we used was GENIE-2K (Canberra Industries, 2006). Each energy spectrum has been recorded for a period of 15 min in order to minimize the statistical error of the peak area (0.3%).

Experimental characterization of any radiation detector usually consists of three calibration stages: energy calibration, resolution calibration and efficiency calibration.

2.1.1. Energy calibration

The energy calibration express the expected proportionality between the channel number *C* and known photon energy *E*.

Nevertheless, in practice, a small degree of nonlinearity in this relationship is often observed in gamma ray measurements (Knoll, 2000) and should be taken into account. Accordingly, in the present work, a second-order polynomial (eq. (1)) was used to establish this non-linearity:

$$E = a' + b'C + d'C^2 \tag{1}$$

The values of *a'*, *b'* and *d'* were calculated by a least-square fit from experimental points. Energy calibration data and curve fit of the 2"x 2" NaI(Tl) detector are shown in Fig. 2.

2.1.2. Resolution curve

The energy resolution of a detector system indicates how well it is able to discriminate gamma photons with similar energies. The intrinsic energy resolution of the scintillator material often dominates the achievable energy resolution of a detector system. The energy resolution, *R*, is defined as the full width at half maximum (FWHM) of the energy peak *E*₀. It is often expressed as a percentage:

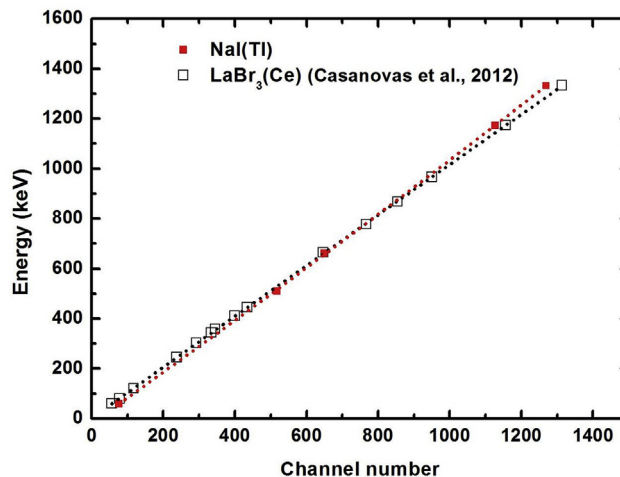


Fig. 2. Energy calibration of the 2"x 2" NaI(Tl) detector. The dashed curve corresponds to a 2nd-order polynomial fit.

$$R = \frac{FWHM}{E_0} \times 100\% \tag{2}$$

The energy resolution function was expressed by a power law relationship

$$R = a E^b \tag{3}$$

where the values of *a* and *b* were determined by a least square fit. Fig. 3 shows the experimental values and curves fits for the energy resolution of the 2"x 2" NaI(Tl) detector (present work) whereas data representing the 2"x 2" LaBr₃(Ce) detector are from reference (Casanovas, Morant, & Salvadó, 2012). As can be expected, the energy resolution of LaBr₃(Ce) detector is superior to that obtained with NaI(Tl) detector of comparable size: i.e. the average energy resolution at 662 keV in the case of LaBr₃(Ce) detector is 2.5% while its value is 8.5% for the NaI(Tl) detector.

2.1.3. Efficiency measurement

For any gamma radiation detector, a formal definition of absolute efficiency, *ε*, is given by the following ratio:

$$\epsilon = \frac{\text{no. of recorded photons}}{\text{no. of photons emitted by source}} \tag{4}$$

Absolute efficiency is dependent not only on detector properties but

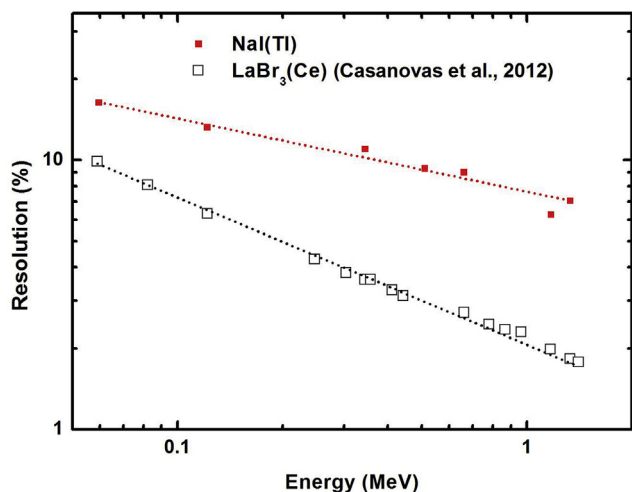


Fig. 3. Experimental values and curves fit for the energy resolution. Data obtained for the 2"x 2" NaI(Tl) detector are indicated with black squares (present work) while open squares represent data from (Casanovas et al., 2012).

on the counting geometry (essentially the source-detector distance, the radiation energy E and the corresponding emission probability) also (Knoll, 2000).

From an experimental standpoint, the absolute efficiency of a detector at energy " E " is expressed by the following formula:

$$\epsilon = \frac{N}{t \cdot P \cdot A} \tag{5}$$

Where N denotes the measured net photopeak area (counts); t is the acquisition time (s); P is the photon emission probability and A denotes the activity of the gamma source at the time of the measurement (Bq).

In practice, the net counts, N , for a particular photopeak is determined by manually setting a region of interest (ROI) around the peak of interest and subsequently the Genie-2K program automatically computes, after background subtraction via a sophisticated algorithm, not only the peak location but the net area also.

Relative uncertainties in the measured efficiency were computed from the uncertainties in emission probability (2–5%), source activity (3%) and statistical error of the peak area (0.3%) (Elanique et al., 2012).

2.2. Monte Carlo simulation

2.2.1. Monte Carlo approach and the MCNP code

Among the most reliable methods for characterizing radiation detectors is the Monte Carlo technique which constitutes, thanks to advances in computer technology, a valid and even preferable alternative to conventional methods (Berger & Seltzer, 1972). One of the advantages of MC method is its ability to perform virtually a "computer experiment" without manipulating any radioactive material and to provide precise computational results. MC calculation however, strongly depends upon the parameters accuracies associated with the detector's geometry and the material composition of the sample (Gardner & Liyanan, 2000).

MC method is particularly suitable for complex geometries where analytical methods cannot be applied. In MC approach, each photon is tracked from creation until death (escape or absorption) with all interactions based on physics models and cross-sections for physics processes (photoelectric absorption, Compton scattering, and pair production) and all decisions, i.e. interaction point location, scattering angle, are based on pseudo-random numbers (Hendricks et al., 2000).

The present simulations were carried out using the Monte Carlo code MCNP-X (Pelowitz, 2005) which nowadays is among the most used MC codes worldwide. As a versatile radiation transport code,

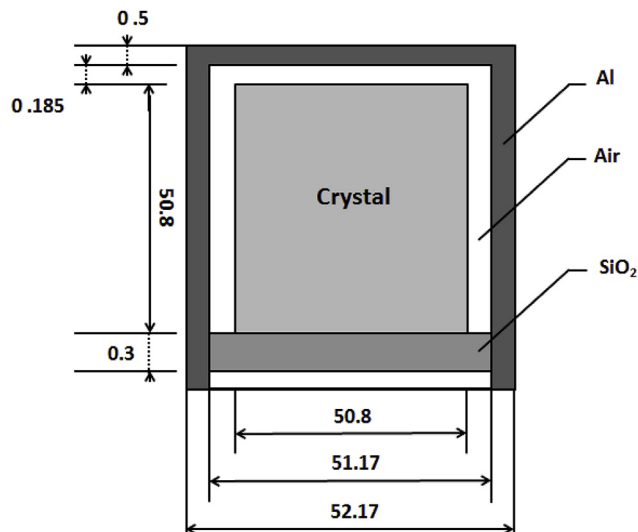


Fig. 4. Inner structure of the 2"x 2" detectors (NaI(Tl) and LaBr₃(Ce)) considered in MC simulation. The MgO reflector, used for NaI(Tl) detector model, has been replaced by "air" in the LaBr₃ case according to (Casanovas et al., 2012).

MCNP is a general purpose with the following main features: powerful source description, flexible tally features, and variance reduction techniques. Further details about the code can be found in (Pelowitz, 2005). In practice, the distribution of the photon energy deposited in a crystal volume (cell) is a pulse height spectrum which can be obtained in MCNP via the "F8" tally. This estimator corresponds to the absolute detector efficiency ϵ gamma ray energy.

2.2.2. Modelling the detectors

Fig. 4 shows the inner structure of the 2"x 2" detectors models (NaI(Tl) and LaBr₃(Ce)) considered in MC simulation. For a scope of comparison, we also carried out MC calculations for a cylindrical 2"x 2" LaBr₃(Ce) detector having the same housing materials. Materials densities used for modelling the detectors are shown in Table 2.

Moreover, The MgO reflector, used in the case of NaI model, was replaced by air in the LaBr₃ model. As we already mentioned in (Mouhti et al., 2017), the SiO₂ layer, which substitutes the PM tube, has a negligible effect on the efficiency calculation since it is located behind the crystal.

To improve simulated spectra, the Gaussian Energy Broadening (GEB) option was enabled. In MCNP code, this broadening is defined by the $FWHM$ or ΔE :

$$FWHM = a + b\sqrt{E} + cE^2 \tag{6}$$

where $FWHM$ is Full Width at Half Medium of the photopeak; E is the incident photon energy (MeV); a , b and c are user provided constants from the fitting function.

3. Results and discussion

3.1. Gamma ray energy spectra

A direct comparison of measured and MC simulated gamma-ray spectra from NaI(Tl) scintillator for ¹³⁷Cs source is shown in Fig. 5. As

Table 2
Densities of materials used in the present MC simulations.

SiO ₂	Air	MgO	Al	LaBr ₃	NaI	Material
0.94	1.22×10^{-3}	2.0	2.7	5.29	3.67	Density (g.cm ⁻³)

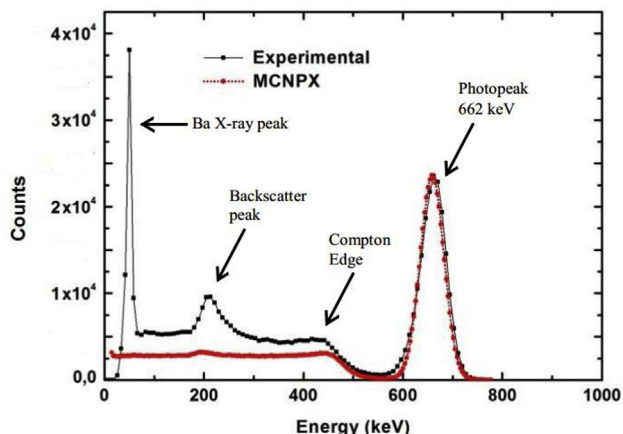


Fig. 5. Comparison of experimentally measured 2''x 2'' NaI(Tl) pulse height spectrum for ¹³⁷Cs source with a theoretical spectrum calculated by MCNP-X code.

previously noticed (Mouhti, Elanique, & Messous, 2017), good agreement between both spectra can be observed at least for the photopeak.

Nevertheless, we observed a systematic difference in the Compton continuum below 600 keV where MC spectra underestimate experimental data. This is most likely due to the photons scattered by surrounding materials (Berger & Seltzer, 1972). Moreover, the Ba X-ray peak at 32 keV (K shell) observed in the measured spectrum was not considered in MC calculations.

To better illustrate the difference between LaBr₃(Ce) and NaI(Tl) scintillators in terms of energy resolution, we have shown in Fig. 6 their pulse height spectra calculated by MCNP-X for ⁶⁰Co source. The energy resolution of LaBr₃ detector (2% at 1117 keV) is clearly enhanced by a factor of ~3.5 circa compared to that of NaI(Tl) detector.

3.2. Efficiency calculations

Fig. 7 shows the absolute efficiency curves for the 2''x 2'' NaI(Tl) detector in the 100–1400 keV range. Comparison between measured efficiencies and MC simulated data showed good agreement which is lower than ± 10% in the investigated energy range.

The efficiency curves of the NaI(Tl) detector, described in section 3.2., were fitted by a polynomial function given by eq. (7):

$$\varepsilon = a + bE + cE^3 \tag{7}$$

where ε denotes the absolute efficiency; E is the photon energy (keV); and the adjustment coefficients, obtained by least squares method, are:

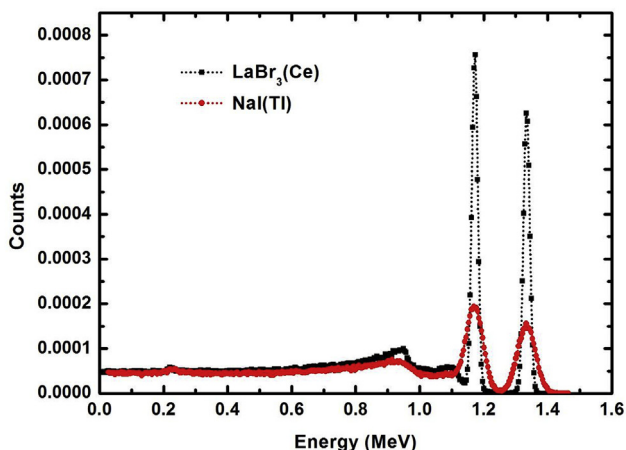


Fig. 6. MC simulated pulse height spectra for LaBr₃(Ce) (square) and NaI(Tl) scintillators (circle) of equal 2''x 2'' size for gamma rays from ⁶⁰Co.

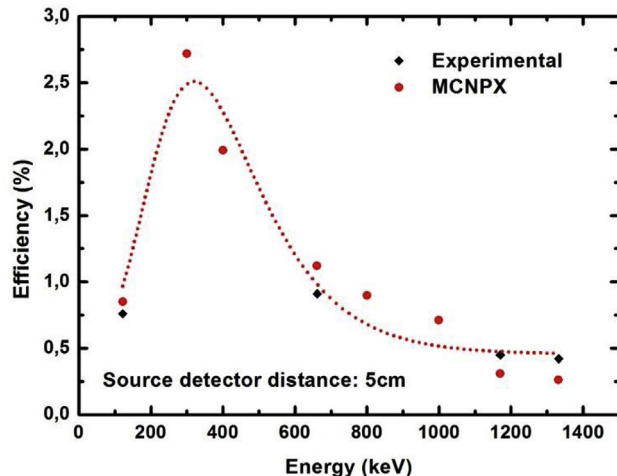


Fig. 7. Measured and calculated efficiencies for the 2''x 2'' NaI(Tl) detector. The source-detector distance was 5 cm.

Table 3

NaI(Tl) detector's efficiency values obtained by MC simulation and measurements. The term RD denotes the relative difference defined by:

NaI(Tl)	Source-detector distance (cm)		Photon energy (keV)
$RD(\%)$	$\varepsilon_{MC}(\%)$	$\varepsilon_{exp}(\%)$	
13.34	13.04	11.3	59.5
10.8	4.79	5.37	121.8
2.3	3.05	2.98	661.6
11.8	1.44	1.27	1173.2
4.72	1.27	1.21	1332.5

Table 4

Comparison of the experimental and the MC simulated efficiencies of LaBr₃(Ce) detector.

LaBr ₃ (Ce)			Source-detector distance (cm)	Photon energy (keV)
$\varepsilon_{MCNP}(\%)$ (present work)	$\varepsilon_{EGS}(\%)$ (Casanovas et al.)	$\varepsilon_{exp}(\%)$ (Casanovas et al.)		
3.95	3.09	3.0	5	59.5
2.34	2.01	2.0	5	302.85
2.05	2.01	1.8	5	356.01
1.45	1.31	1.3	5	661.6
2.48	2.15	2.1	2	1173.2
2.20	1.90	2.0	2	1332.5

a , b and c .

To validate the mathematical models of the studied scintillators, we compared MC simulated efficiencies to measured values for the 2''x 2'' NaI(Tl) (Table 3) and for the 2''x 2'' LaBr₃(Ce) (Table 4).

In the case of LaBr₃ detector (Table 4), the efficiency data were reproduced from (Casanovas et al., 2012), whereas MCNP simulation indicates present work. Our MCNP calculations were also compared to MC results of (Casanovas et al., 2012) using the EGS Monte Carlo code.

The results of both Table 3 and Table 4 show that the simulated efficiency values are in good agreement with those measured. Nevertheless, the largest discrepancy of 13.34% was found to be for the 59.5 keV photon energy from ²⁴¹Am, where empirical efficiency was underestimated with respect to MC value. This could be explained by the significant process of self-absorption within the source of low-energy photons. Such results are also consistent with (Salgado, Brandão, Schirru, Pereira, & Conti, 2012).

4. Conclusion

In this study, the Monte Carlo simulation computer code MCNP was used to provide a precise mathematical model of two scintillation detectors with similar size $2'' \times 2''$: NaI(Tl) and LaBr₃(Ce) detectors. The photon detection efficiency and energy resolution curve were measured for the NaI(Tl) detector in the gamma energy range from 60 keV to 1408 keV. Comparison of the experimental efficiency values with MCNP simulations results for each detector showed good agreement. Nevertheless, the largest discrepancy of 13.34%, in the case of NaI(Tl) detector, was observed for the 60 keV photon from the ²⁴¹Am source. The later would be explained by self-attenuation of low photon energy within the source.

This comparison has enabled us the validation of the developed mathematical model for both NaI(Tl) and LaBr₃(Ce) scintillators. The present study showed that Monte Carlo simulation programs provide a very useful, efficient and reliable tool for mathematical detector calibration.

Declarations of interest

None.

Funding source

This research did not receive any specific grant from funding agencies in the public, commercial, or not-for-profit sectors.

References

- Berger, M. J., & Seltzer, S. M. (1972). Response functions for sodium iodide scintillation detectors. *Nuclear Instruments and Methods*, 104(2), 317–332.
- Canberra Industries Inc (2006). *Genie 2000 spectroscopy software manual v. 3.1*.
- Casanovas, R., Morant, J. J., & Salvadó, M. (2012). Energy and resolution calibration of NaI(Tl) and LaBr₃(Ce) scintillators and validation of an EGS5 Monte Carlo user code for efficiency calculations. *Nuclear Instruments and Methods in Physics Research Section A: Accelerators, Spectrometers, Detectors and Associated Equipment*, 675, 78–83.
- Elanique, A., Marzocchi, O., Leone, D., Hegenbart, L., Breustedt, B., & Oufni, L. (2012). Dead layer thickness characterization of an HPGe detector by measurements and Monte Carlo simulations. *Applied Radiation and Isotopes*, 70, 538–542.
- Ewa, I. O. B., Bodizs, D., Czifrus, S. Z., & Molnar, Z. S. (2001). Monte Carlo determination of full energy peak efficiency for a HPGe detector. *Applied Radiation and Isotopes*, 55, 103–108.
- Gardner, R. P., & Lianyan, Liu (2000). Monte Carlo simulation for IRRMA. *Applied Radiation and Isotopes*, 53, 837–855.
- Hendricks, J. S., Adams, K. J., Booth, T. E., Briesmeister, J. F., Carter, L. L., Coxa, L. J., et al. (2000). Present and future capabilities of MCNP. *Applied Radiation and Isotopes*, 53, 857–861.
- Knoll, G. F. (2000). *Radiation detection and measurement* (4th ed.). New York: Wiley (Chapter 8).
- Mouhti, I., Elanique, A., & Messous, M. Y. (2017). Monte Carlo modelling of a NaI(Tl) scintillator detectors using MCNP simulation code. *Journal of Materials and Environmental Science*, 8(12), 4560–4565.
- Pelowitz, D. B. (2005). *MCNP-x User's manual, version 2.5.0 LA-CP-05-0369*. Los Alamos National Laboratory.
- Saizu, M. A., & Cata-Danil, G. (2011). Lanthanum Bromide scintillation detector for gamma spectrometry applied in internal radioactive contamination measurements. *Scientific Bulletin (ISSN (online) 2286-3672), Series A*, 73(4), 119–126.
- Salgado, C. M., Brandão, L. E. B., Schirru, R., Pereira, C. A., & Conti, C. C. (2012). Validation of a NaI(Tl) detector's model developed with MCNP-X code. *Progress in Nuclear Energy*, 59, 19–25.
- Sonzogni, A. A. (2003). Nuclear data Sheets for A = 138. *Nuclear Data Sheets*, 98, 515–664.